Eur. Phys. J. C (2016) 76:194
DOI 10.1140/epjc/s10052-016-4031-y

THE EUROPEAN PHYSICAL JOURNAL C

Regular Article - Experimental Physics

QED radiative corrections and their impact on $H \to \tau\tau$ searches at the LHC

Mieczyslaw Witold Krasny[1,a], **Stanisław Jadach**[2], **Wiesław Płaczek**[3]

[1] Laboratoire de Physique Nucléaire et des Hautes Energies, Université Pierre et Marie Curie-Paris 6, Université Paris Diderot-Paris 7, CNRS-IN2P3, 4 pl. Jussieu, 75005 Paris, France
[2] Institute of Nuclear Physics, Polish Academy of Sciences, ul. Radzikowskiego 152, 31-342 Kraków, Poland
[3] Marian Smoluchowski Institute of Physics, Jagiellonian University, ul. Łojasiewicza 11, 30-348 Kraków, Poland

Received: 15 February 2016 / Accepted: 17 March 2016 / Published online: 9 April 2016

Abstract In this paper we show that the excess of the $\tau\tau$ events with respect to the Standard Model background predictions, observed by the ATLAS and CMS collaborations and interpreted as the evidence of the Higgs-boson decay into a pair of τ-leptons, may be accounted for by properly taking into account QED radiative corrections in the modelling of the $Z/\gamma^* \to \tau\tau$ background.

1 Introduction

The extraction of a $H \to \tau\tau$ signal from the measured mass spectrum of $\tau\tau$ pairs produced at the Large Hadron Collider (LHC) requires very precise knowledge of the expected $H \to \tau\tau$ and $Z/\gamma^* \to \tau\tau$ mass spectra. If the mass of the $\tau\tau$ pairs is reconstructed with perfect resolution then analysis is simple. However, in reality the analysis is complicated by the missing energy carried by neutrinos from τ-decays, the resolution of the measurements of the energies of the various particles in the final state, and, last but not the least, the adequate modelling of the photon radiation processes.

In this paper we discuss the robustness of experimental evidence of the $H \to \tau\tau$ decays extracted from data collected at the LHC – reported by the ATLAS and CMS collaborations [1,2] and considered as the direct confirmation of the Higgs-boson coupling to fermions. We focus our investigation on the processes of radiation of photons by muons and τ-leptons. These processes become particularly important for the Higgs-signal search strategy in which the dominant $Z/\gamma^* \to \tau\tau$ background is modelled using $Z/\gamma^* \to \mu\mu$ events. This modelling, customarily called *the embedding procedure*, was used by both the ATLAS and CMS collaborations in their respective analyses [1,2].

The embedding procedure exposes the analyses to the necessity of taking into account and applying the QED radiative corrections, which are specific to this procedure. The study presented in this paper demonstrates that they are large and could explain all the excess of events interpreted as the $H \to \tau\tau$ signal.

This paper is organised as follows. The ATLAS and CMS embedding procedure is summarised in Sect. 2. Section 3 starts with an introductory discussion of the radiative corrections to the Z/γ^*-boson leptonic decays. This discussion is followed by a presentation of the Monte Carlo tools used in the analysis of the QED radiative processes associated with the Z/γ^*-boson decays into τ and μ pairs. We analyse the dependence of radiative corrections on the assumed parton distributions, fragmentation model, handling of processes involving multi-photon emissions, in order to asses the theoretical precision of the results presented in subsequent sections of this paper. Finally, in Sect. 3 we discuss the size of the radiative corrections for an analysis based on the embedding procedure and its dependence on the experimental resolution of the reconstructed invariant mass of $\tau^+\tau^-$ pairs. In Sect. 4 we present our predictions for the excess of events by properly taking into account radiative photons in the modelling of the $Z/\gamma^* \to \tau\tau$ background. We compare this excess with that of the predicted Higgs-boson signal. In our study we follow the published ATLAS and CMS analyses [1,2]. In Sect. 5 we discuss why the radiative corrections effects were not given sufficient attention in the ATLAS and CMS analyses. In Sect. 6 we propose a list of tests that can check experimentally the size of the radiative correction effects and discriminate between signatures of Higgs-boson

The work is partly supported by the program of the French–Polish co-operation between IN2P3 and COPIN No. 05-116, and by the Polish National Centre of Science Grant No. DEC-2012/04/M/ST2/00240.

[a] e-mail: krasny@lpnhe.in2p3.fr

decays versus missing radiative corrections in the modelling of the $Z/\gamma^* \to \tau\tau$ background. The conclusions of the paper are presented in Sect. 7.

2 Modelling of $Z/\gamma^* \to \tau\tau$ processes with τ-embedded $Z/\gamma^* \to \mu\mu$ events

The $\tau\tau$-decays of Z/γ^*-bosons produced by the Drell–Yan process are the dominant source of background for $H \to \tau\tau$ searches at the LHC. The background evaluation method is common for both ATLAS and CMS analyses [1,2]. The $Z/\gamma^* \to \tau\tau$ decays are modelled using *embedded event samples* in loosely selected $Z/\gamma^* \to \mu\mu$ data. These event samples are recorded for each data taking period. In the embedding procedure muon tracks and their associated energy depositions in the calorimeters are replaced by a simulated detector response to the final-state particles of the corresponding τ-lepton decays.

In deriving the momentum vectors of the embedded τ-leptons, the momentum vectors of the corresponding muons are used. These vectors are determined using the muon tracks reconstructed from the central tracker and muon spectrometer hits. The τ-momentum vectors are calculated by taking the energies of the corresponding muons and correcting the μ-momentum vectors for the effect of the muon and τ-lepton mass difference. The energy depositions in the calorimeter which are identified as being associated with the outgoing muons are removed. Next, the detector response to the τ-leptons is simulated. In the initial simulation step the radiation of photons and the decays of τ-leptons are generated. In the final step the response of the tracker and of the calorimeters to the τ-lepton decay products are simulated.

There are several advantages of the embedding technique: the sensitivity to the Monte Carlo modelling aspects of the hadronic system associated with the Z/γ^*-boson production is minimised, the pile-up effects are automatically taken into account in the background simulation, including the underlying event activity. However, as discussed in the next section, there is a price to pay for such a simplification of the background estimation technique.

3 Radiative corrections in Z/γ^* leptonic decays

3.1 Initial discussion

Leptons produced in Z/γ^*-boson decays radiate photons. The probability of radiation depends on the lepton mass. Electrons radiate photons more frequently than muons, muons more frequently than τ-leptons. The difference of probabilities is proportional to the logarithm of the squares of the leptons masses, $(\alpha/\pi)\ln(m_i^2/m_j^2)$.

In order to describe the observed invariant mass distributions of pairs of leptons produced in Z/γ^*-decays, the processes of final-state photon radiation (FSR) have to be modelled and the corresponding radiative corrections should be taken into account.

The size of the radiative corrections depends not only on the lepton type, but also on the lepton detection apparatus, the experimental cuts and the reconstruction method of the lepton momentum vector. Radiative corrections for the measurements of the lepton momentum which include information of radiated photons reconstructed in the calorimeter are sizeably smaller than those based on its momentum vector solely measured from the curvature of the lepton track.

In this paper we use the term *bare leptons* for those which have their momentum vector reconstructed solely from the track parameters and the term *dressed leptons* for an idealised case in which all the radiative photons are assigned to their lepton emitters and the photon measured momenta are used in the reconstruction of the initial momentum vector of the leptons.[1] The radiative corrections for the bare-lepton-based measurements are large, while the ones based on the dressed leptons are small. In general, the size of the radiative corrections may vary within the above boundaries. Their numerical values are detector- and analysis-dependent, and reflect the efficiency of algorithms, which assign the photon energy depositions in the calorimeters to the respective outgoing leptons.

The photon radiation by τ-leptons has an additional subtlety with respect to photon radiation by stable electrons and long-lived muons. Photons may originate both from the τ-lepton radiation and from the τ decays. Since neutrinos produced in the τ decays remain undetected, it is hardly possible to experimentally identify the photon origin on an event-by-event basis from the reconstructed τ-mass.

At first sight the QED radiative effects should play a negligible role in the determination of the strength of the $H \to \tau\tau$ decay signal. This is perhaps why the necessity to evaluate the radiative correction to the embedding procedure escaped attention. As discussed in Sect. 3.3, these corrections, for a realistic detector resolution and for the adapted measurement strategy, are large and cannot be neglected.

In advance of a quantitative analysis of the radiative corrections to the embedding procedure, we first present the Monte Carlo tools used in our analysis and evaluate their precision.

3.2 Theoretical control

The inclusive cross section for the $H \to \tau\tau$ decays is, in the LHC energy range, three orders of magnitude lower than that

[1] Such an association, to be exact, can only be made at the amplitude, rather than cross-section level.

for $Z/\gamma^* \to \tau\tau$ decays. This 10^{-3} ratio defines the precision *yard-stick* for the requisite theoretical and experimental control of the $Z/\gamma^* \to \tau\tau$ background.

In the studies presented in this paper we use the Monte Carlo event generator WINHAC [3–6]. This program simulates the single $W^{\pm}/Z/\gamma^*$-boson production with leptonic decays in hadronic collisions, i.e. the charged-current (CC) and neutral-current (NC) single Drell–Yan (DY) processes. The parton-level hard processes are convoluted with parton distribution functions (PDFs) supplied through the LHAPDF library [7]. For the W-boson processes WINHAC features the $\mathcal{O}(\alpha)$ Yennie–Frautschi–Suura (YFS) exclusive exponentiation for the electroweak corrections [4–6]. This is not the case for the Z/γ^* processes, considered in this paper, which are included only at the Born level and the QED radiative corrections are provided through an interface to the PHOTOS generator [8–11]. PHOTOS generates multi-photon final-state radiation (FSR) in Z/γ^* decays with the use of an iterative algorithm in which resummation of leading QED radiative effects is improved with a matrix-element (ME) correction to account for sub-leading, mainly $\mathcal{O}(\alpha)$, effects. It is shown in Ref. [12] that PHOTOS reproduces very well the exact $\mathcal{O}(\alpha)$ FSR corrections. In this paper we refer to the generator based on the WINHAC and PHOTOS interface as WINHAC+PHOTOS.

WINHAC includes only the leading-order (LO) QCD matrix elements. However, in order to generate realistic kinematical distributions of Z/γ^*, it is interfaced with the PYTHIA 6.4 generator [13], which performs the initial-state QCD (and QED) parton shower, the appropriate proton-remnant treatment and the necessary hadronisation/decays. This interface provides an improved generation of lepton transverse momenta with respect to the original PYTHIA 6 program, which results in a good agreement with the NLO QCD predictions; for details see Ref. [14].

In the studies presented in this paper we use as the baseline the CTEQ6.1 parametrisation of PDFs [15]. Other parametrisations, such as MSTW2008NNLO [16], are considered as a cross-check of the PDF-dependence of the Z/γ^* kinematical distributions.

For our studies of the QED FSR effects we use PHOTOS in its best set-up, i.e. with multi-photon radiation including the ME correction. To see how important are the sub-leading $\mathcal{O}(\alpha)$ FSR corrections we also perform computations with the ME correction switched off. In order to cross-check the WINHAC+PHOTOS results, we use the KKMC Monte Carlo event generator [17]. It features the $\mathcal{O}(\alpha^2)$ YFS exclusive exponentiation of QED radiative corrections in the process of Z/γ^* production and decay. Its main advantages with respect to PHOTOS are: inclusion of initial-final state radiation interferences, the exact $\mathcal{O}(\alpha^2)$ FSR corrections and a better overall normalisation (includes the radiative corrections, which is not the case in PHOTOS). Initially KKMC was developed for e^+e^- colliders, such as LEP, but recently it has been adapted also for hadron colliders by adding quark beams and a possibility of their convolution with PDFs. It was already used to assess the size of the second-order QED correction to the ϕ^*_η observable for the NC DY process at the LHC [18].

Since we want to follow closely the analysis of the LHC experiments, instead of using the QCD K-factors, we normalise the Z/γ^*-boson and Higgs-boson cross sections to the values used in the ATLAS analysis [1].

The analysis shown in the current and in the following sections is made for the pp centre-of-mass collision energy of 8 TeV and the event-acceptance cuts:

$$|\eta_l| \leq 2.5, \quad p_{T,l} \geq 10\ \text{GeV}, \quad m_{ll} \geq 40\ \text{GeV}, \tag{1}$$

where η_l, $p_{T,l}$ and m_{ll} are, respectively, the pseudo-rapidity, the transverse momentum of each of the leptons ($\mu^{\pm}$ or $\tau^{\pm}$) and the invariant mass of the opposite-sign lepton pairs.

In Fig. 1 we present the results of the generator-level precision evaluation of the tools used in this analysis. In Fig. 1a we show the Born-level invariant-mass distribution of the $\tau^+\tau^-$ pairs which originate from Z/γ^*-boson decays and from Higgs-boson decays. At the event generator level the Higgs-boson peak is clearly visible above the Z/γ^*-boson background.

The QED FSR corrections ($\delta = \frac{d\sigma_{\text{FSR}}}{d\sigma_{\text{Born}}} - 1$) to the bare-dilepton invariant mass distribution m_{ll}, for the Z/γ^* decays, are shown in Fig. 1b, separately for τ-pair and for μ-pair final states. As expected, the radiative corrections for the τ case are significantly (∼2 times) smaller than those for the μ case. The FSR corrections are positive below the Z-boson mass peak and can be as large as ∼100 % for muons and ∼50 % for taus. At $m_{ll} = M_Z$ the corrections change sign and become negative. In the Higgs-boson region (∼125 GeV) the corrections are about −10 % for muons and about −5 % for taus.

In Fig. 1c we show that the sensitivity of a realistic simulation of the Z/γ^*-boson four-momentum for μ-pair final states to PDF parametrisations and to PYTHIA parton-shower and hadronisation effects is small. We use CTEQ6.1 PDFs with and without PYTHIA, and MSTW2008NNLO PDFs with PYTHIA. As can be seen, all three curves are on top of each other. Clearly, the results for the FSR corrections do not depend, within a 1 %, on the QCD patron-shower and hadronisation effects, or on the choice of the PDFs parametrisation.

Finally, in Fig. 1d, we present the study of effects of various approximations used in the calculations of the QED radiative corrections. We compare two running modes of PHOTOS: (1) its best set-up, i.e. multi-photon radiation including the ME correction, denoted as PHOTOS-Best, and (2) the multi-photon radiation without the ME correction, denoted as PHOTOS-LL. The differences between these two

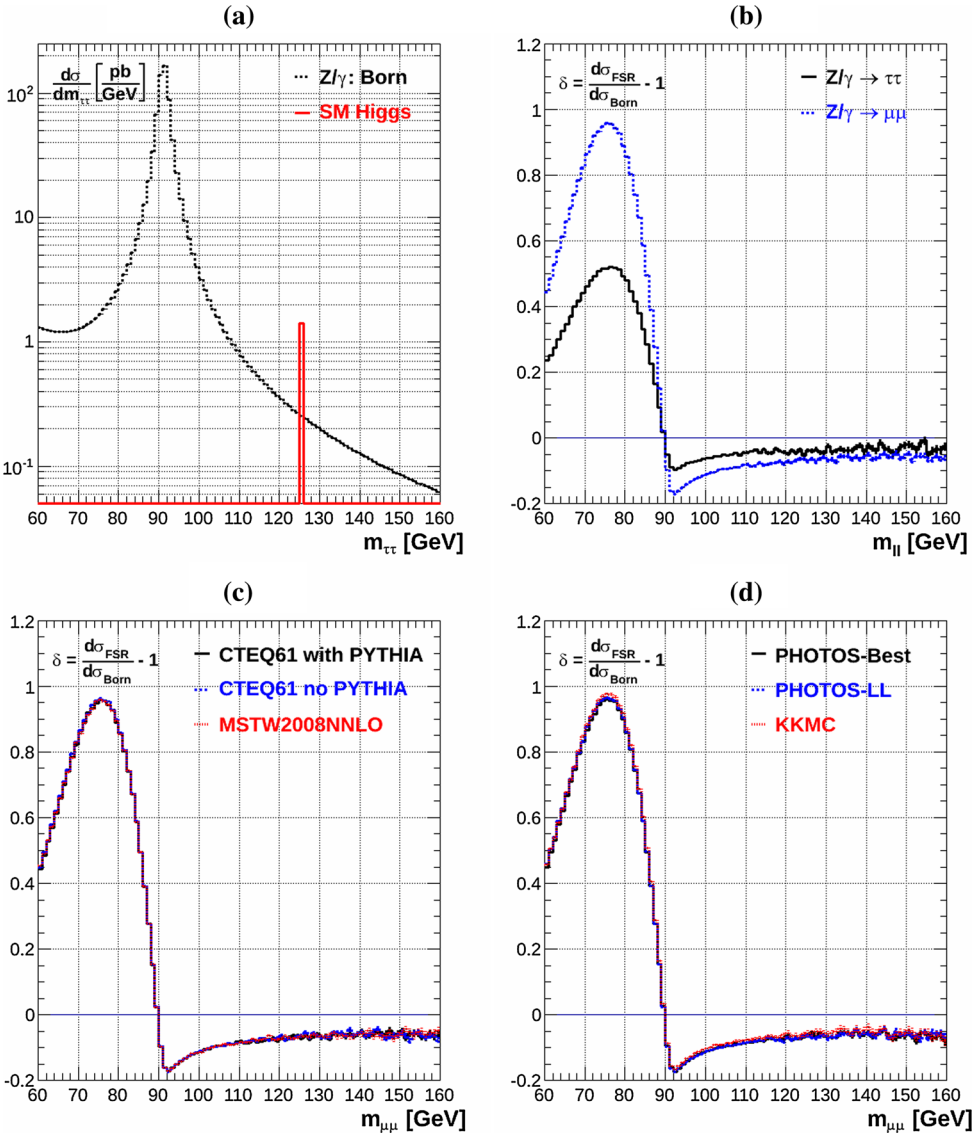

Fig. 1 **a** The WINHAC+PHOTOS inclusive opposite sign $\tau\tau$ mass distribution and the expected 125 GeV Standard Model Higgs signal (shown for a bin width of 1 GeV); **b** the QED radiative corrections ($\delta = \frac{d\sigma_{\rm FSR}}{d\sigma_{\rm Born}} - 1$) for bare μ and τ pairs; **c** the PDF and QCD-effects dependence of the size of the QED radiative corrections for the muon pairs (see text for details); **d** the size of the QED radiative corrections for various calculation approximations (see text for details)

results are very small, below 1 %, and are not visible in the plot. This shows that the ME correction in PHOTOS, which accounts for the sub-leading $\mathcal{O}(\alpha)$ QED effects, is not important for the studies presented here. Nevertheless, our main results are obtained using PHOTOS in its best set-up. In Fig. 1d, we also compare the WINHAC+PHOTOS radiative corrections with those of KKMC. Here the differences are also barely visible in the plot: they reach up to 1.5 % below the Z-boson mass peak and up to ∼1 % above it. These can be attributed to the differences between KKMC and PHOTOS discussed earlier. We have checked that these differences are almost identical for the τ and μ cases. Therefore, as far as the difference of the radiative corrections for muons and taus is concerned, they are negligible. The same is true for the purely weak corrections. Therefore, we conclude that WINHAC+PHOTOS is adequate for our study of the QED FSR influence on the background to the $H \to \tau\tau$ signal in the LHC Run 1 data. In the future, with increased statistical and systematic precision of the LHC data, using more precise MC generators, such as KKMC, may be necessary.

The above study demonstrates that at the generator level the radiative corrections for the NC DY process are well controlled. In the mass region relevant for the Higgs signal they are small compared to the signal itself. One could thus expect that they would have a negligible impact on the experimental determination of the $H \to \tau\tau$ signal at the present statistical precision. This is indeed the case for the classical analysis, in which the radiative effects are implemented in all the background MC generators and the treatment of simulated and data events is the same.

In the following subsection we demonstrate that this statement no longer holds for the embedding-procedure-based analysis which uses real rather than generated events.

3.3 FSR corrections to embedding procedure

As discussed earlier, we use the term *bare leptons* for those which have their momentum vector reconstructed solely from the track parameters and the term *dressed leptons* for an idealised case in which all the radiative photons are assigned to their lepton emitters and the photon measured momenta are used in the reconstruction of the initial momentum vector of the leptons. Therefore the dressed lepton, as far as the FSR is concerned, is equivalent to a Born lepton. If in the extraction of the Higgs signal, data are compared to complete Monte Carlo simulations of $Z/\gamma^* \to \tau\tau$ and $H \to \tau\tau$ events, the analysis would be consistent. In the analyses of [1,2] a fully simulated $H \to \tau\tau$ sample is used. However, the $Z/\gamma^* \to \tau\tau$ sample is obtained by embedding τ-leptons in a sample of $Z/\gamma^* \to \mu\mu$ data. Had dressed τ-leptons been used to replace dressed muons in data, the analysis would still be consistent. However, what is done instead, is to replace bare muons in data with simulated dressed τ-leptons.

The necessity of taking into account the QED FSR corrections to the embedding procedure has its origin in the interplay of the following three effects:

- in the embedding procedure bare muons in data are replaced by simulated dressed τ-leptons,
- the measurement resolution of the invariant mass of two opposite-charge τ-leptons ($\tau^+\tau^-$) is comparable to the mass difference between the Z-boson and the Higgs boson,
- the inclusive cross section for Z/γ^*-bosons decaying into leptons is three orders of magnitude larger than that for the Higgs boson.

The interplay of the above three effects is illustrated in Fig. 2. The upper left plot (a), shows the difference between the WINHAC+PHOTOS differential cross section plotted as a function of the invariant mass of the $\tau^+\tau^-$ pair, $m_{\tau\tau}$, for the generated sample of the $Z/\gamma^* \to \tau\tau$ decays and for the corresponding cross section for the case, where the τ-lepton momenta are determined using the embedded $Z/\gamma^* \to \mu\mu$ sample. We call the differential cross-section difference:

$$\frac{\Delta d\sigma}{dm_{\tau\tau}} = \frac{d\sigma_{\text{generated}}}{dm_{\tau\tau}} - \frac{d\sigma_{\text{embedded}}}{dm_{\tau\tau}}, \tag{2}$$

the radiative corrections to the embedding procedure. Note, that these corrections are additive rather than multiplicative. Such a representation is appropriate for the studies of radiative corrections which are "non-local", i.e. for the case when their size in each mass bin is an integral over the Born cross section for a wide mass interval.

The procedure of association of the radiative photons with the parent τ-leptons in the reconstruction is not discussed in [1,2]. Therefore, we cannot provide in this paper a precise estimate of the radiative corrections to the embedding procedure. Instead, we estimate upper and lower boundaries of the radiative corrections. Below we refer to these two boundaries as (1) *dressed corrections*, and (2) *bare corrections*.

The two distributions shown in Fig. 2a reflect the following two possible outcomes of the reconstruction of the outgoing τ-lepton momenta in generated $Z/\gamma^* \to \tau\tau$ decays: (1) the momenta of the dressed τ-leptons – represented by the dashed line (dressed corrections) and (2) the momenta of the bare τ-leptons – represented by the dots (bare corrections). These correspond to boundaries on the size of the radiative corrections to the embedding procedure.

If, in the event-by-event experimental reconstruction procedure of the τ-lepton momenta, all photons radiated by each of the τ-leptons were reconstructed from the electromagnetic energy clusters in the calorimeters and if they were unambiguously associated to one of the outgoing τ-leptons, contributing to its momentum reconstruction, the radiative corrections would be those represented by the dashed line. If, on the other hand, all the calorimetric energy depositions of photons coming from the initial τ-lepton radiation (before its decay) were not associated to their parent τ-leptons, the radiative corrections to the embedding procedure would have the values represented by the dots.

The solid line in Fig. 2a represents the cross section for the $H \to \tau\tau$ decay signal for the case of perfect resolution. It is significantly higher than the size of the radiative corrections. Thus, are the radiative corrections irrelevant while establishing the existence of the Higgs-boson signal? If the invariant mass of the τ-lepton pairs, $m_{\tau\tau}$, could be reconstructed with the precision comparable to that for the muon pairs, the answer would be affirmative and the discussion in this chapter could be considered as purely academic. In reality, however, the mass of the τ-lepton pairs is reconstructed with finite resolution, insufficient to assign the τ-lepton pairs to either the Z/γ^*-boson or Higgs-boson source, on an event-by-event basis.

In Fig. 2b–d we show the size of the radiative correction to the embedding procedure for the following three values of $\sigma^{\text{smear}}_{m_{\tau\tau}}$ specifying the Gaussian smearing of the reconstructed $m_{\tau\tau}$: $\sigma^{\text{smear}}_{m_{\tau\tau}}$ = 10, 20 and 30 GeV. Already for the $\sigma^{\text{smear}}_{m_{\tau\tau}} = 10$ GeV smearing, the values of the radiative corrections in the mass region of 110–140 GeV are comparable to the Higgs-boson signal. The size of the corrections increases rapidly, in the Higgs signal mass region, with worsening resolution (increasing $\sigma^{\text{smear}}_{m_{\tau\tau}}$), outweighing the Higgs-boson signal already for $\sigma^{\text{smear}}_{m_{\tau\tau}} = 20$ GeV. We recall that these plots were made for the inclusive event sample specified by the kinematical cuts defined in the previous section. It is evident that, for any realistic detector and, in particular, in the presence of escaping neutrinos, these corrections must be considered with great care.

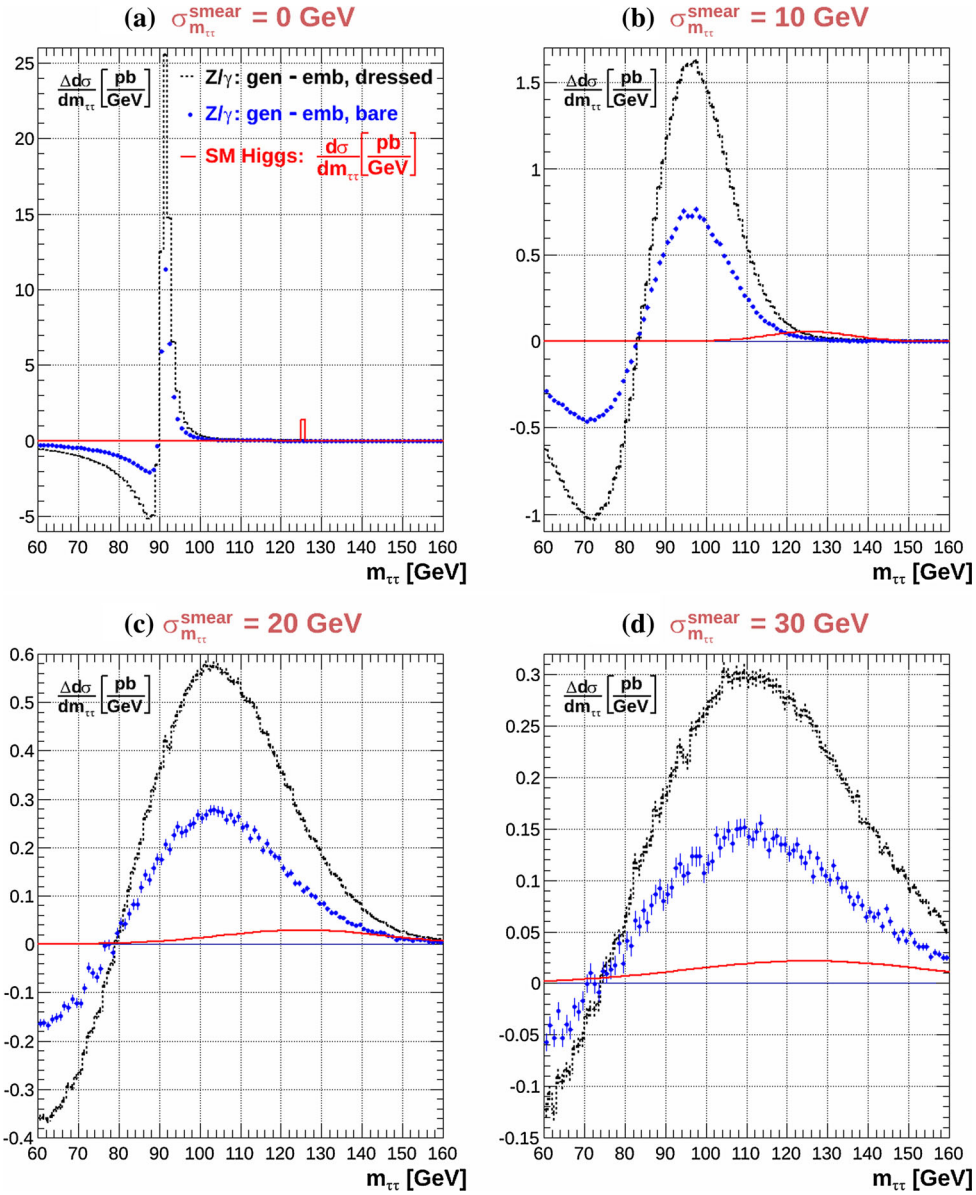

Fig. 2 The dressed and bare QED radiative corrections to the embedding procedure, $\frac{\Delta d\sigma}{dm_{\tau\tau}} = \frac{d\sigma_{\text{generated}}}{dm_{\tau\tau}} - \frac{d\sigma_{\text{embedded}}}{dm_{\tau\tau}}$, for pp centre-of-mass collision energy of 8 TeV and the following event-acceptance cuts: $|\eta_l| \leq 2.5$, $p_{T,l} \geq 10$ GeV and $m_{ll} \geq 40$ GeV. Shown are plots for the following four values of $\sigma^{\text{smear}}_{m_{\tau\tau}}$ specifying the Gaussian smearing of the measured invariant mass of the $\tau^+\tau^-$ pairs: $\sigma^{\text{smear}}_{m_{\tau\tau}} = 0$, 10, 20 and 30 GeV – shown in panels **a**, **b**, **c** and **d**, respectively. The corresponding smeared distributions for the Standard Model (SM) Higgs-boson signal, $\frac{d\sigma}{dm_{\tau\tau}}$, are also shown for comparison

It is also important to note that the radiative corrections to the embedding procedure have a positive sign in the mass region above the Z-boson mass peak and a negative sign below it. If not taken into account, the $Z/\gamma^* \to \tau\tau$ background to the Higgs searches, determined using the embedding procedure, would be significantly (with respect to the Higgs-boson signal strength) underestimated in the Higgs-boson mass search region above Z-boson mass and overestimated for masses smaller than the Z-boson mass. It is thus precisely in the region where $H \to \tau\tau$ decay signals have been reported [1,2] that the neglected radiative corrections to the embedding procedure may potentially produce a spurious Higgs-boson signal by underestimating the background level.

4 $H \to \tau\tau$ evidence

4.1 Initial remarks

The ATLAS and CMS papers discussing the $H \to \tau\tau$ decay evidence [1,2] do not present unfolded signal and background distributions in which the detector and analysis dependent corrections are accounted for. The results presented in such a form cannot, strictly speaking, be fully checked by any external analysis. The goal of the analysis presented in this section is only to provide the best possible *initial estimate* of the size of the missing radiative corrections in the modelling of the $Z/\gamma^* \to \tau\tau$ background and an initial assessment of their impact on the extraction of the

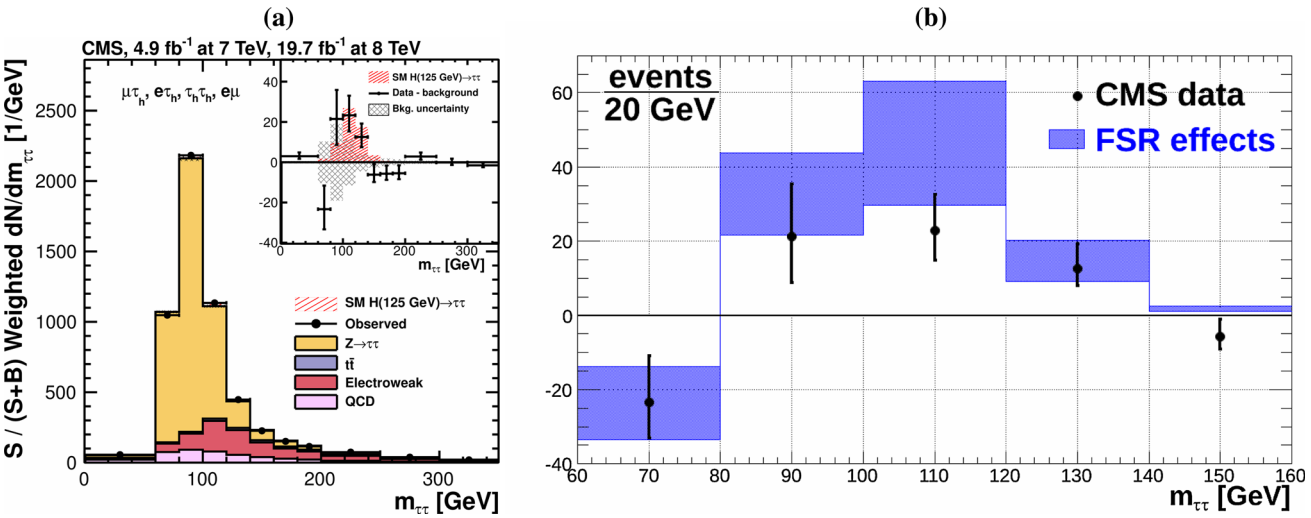

Fig. 3 **a** The CMS Fig. 11 taken from [2]; **b** the comparison of the observed excess of weighted events, interpreted in [2] as the Higgs signal, with our predictions for the for the excess of weighted background events that originate from the missing FSR corrections to the embedding procedure of modelling the $Z/\gamma^* \to \tau\tau$ background

$H \to \tau\tau$ decay signal. Since several simplifications have to be made, we specify the details of these estimates, leaving to the LHC collaborations the precise determination of the size of the corrections for their respective analysis methods.

As discussed in the previous section, the effective size of the missing radiative corrections in the modelling of the $Z/\gamma^* \to \tau\tau$ background for the ATLAS and CMS analyses are sensitive to the experimental resolution of the measurement of $m_{\tau\tau}$. The corrections also depend on the efficiencies of the event-subsample selection cuts, which were optimised in the ATLAS and CMS analyses [1,2] to enrich the $H \to \tau\tau$ signal with respect to all background contributions.

The event-subsamples in the $H \to \tau\tau$ searches are classified in terms of event categories. These categories are characterised by: (1) the type of the τ-lepton decays: $\tau_e(\tau_\mu)\tau_{had}$, $\tau_e\tau_\mu$, $\tau_{had}\tau_{had}$, and (2) the event jet activity and the jet(s) transverse momentum. CMS considers 38 event categories, while ATLAS considers 6 categories (more information on the event categories can be found in Refs. [1,2]). In each of the event categories the $m_{\tau\tau}$ resolution and the ratio of the signal to background are different.

4.2 The CMS case

In Fig. 3a we reproduce Fig. 11 of the CMS paper [2]. Figure 3a shows the observed and predicted $m_{\tau\tau}$ distribution integrated over all the CMS event categories. The normalisation of the predicted background distributions corresponds to the result of a global fit. The Higgs-signal distribution is normalised to the Standard Model (SM) prediction ($\mu = 1$). The distributions in each category, i, are weighted by the ratio between the expected signal and "signal+background" yields, $w_i = S_i/(S_i + B_i)$. The insert shows the corresponding difference between the data and their estimate of the background distributions. Also shown is the expected distribution for a 125 GeV Standard Model Higgs boson.

We estimate the effect of the missing radiative corrections to the embedding procedure in the modelling of the $Z/\gamma^* \to \tau\tau$ background in three steps.

In the first step we determine, from Fig. 3a, the total number of weighted $Z/\gamma^* \to \tau\tau$ events in the mass interval: 60–160 GeV to be $N^w_{tot} = 3780 \pm 190$. In the second step we determine the Gaussian smearing parameter $\sigma^{\rm smear}_{m_{\tau\tau}}$(CMS) of the $m_{\tau\tau}$ measurement as the average of the 38 RMS values, σ_i, for each of the CMS event categories: $\sigma^{\rm smear}_{m_{\tau\tau}}({\rm CMS}) = \langle\sigma_{\rm i}\rangle = 18.4$ GeV. The values for each of the event categories are taken from Table 4 in Appendix B of Ref. [2]. In the third step we calculate our predictions for the QED radiative corrections to the $Z/\gamma^* \to \tau\tau$ background contribution shown in Fig. 3a.

We first calculate the difference between the differential cross section for the generated sample of $Z/\gamma^* \to \tau\tau$ decays and the corresponding cross section in which the τ-lepton momenta are determined by using the embedded $Z/\gamma^* \to \mu\mu$ sample. We do it twice: for the bare and for the dressed lepton corrections with the Gaussian mass smearing of $\sigma^{\rm smear}_{m_{\tau\tau}}({\rm CMS}) = 18.4$ GeV. The cross sections are subsequently multiplied by the "weighted" luminosity defined such that the total number of the embedded $Z/\gamma^* \to \tau\tau$ events in the mass internal 60–160 GeV is equal to the number of the weighed events in the CMS data, N^w_{tot}. This normalisation allows us to replace the calculation of the radiative corrections to the differential cross sections by the calculation of the number of weighted events which must be added to

the $Z/\gamma^* \to \tau\tau$ background contribution, shown in Fig. 3a, in order to take into account the missing radiative corrections in the modelling of the $Z/\gamma^* \to \tau\tau$ background.

Such a procedure involves the following three simplifications:

1. The $m_{\tau\tau}$ smearing is assumed to be Gaussian.
2. The small effect of the radiative corrections to the category dependent weights, w_i, which requires their redefinition as $w_i^{'} = S_i/(S_i + B_i(1+\delta_i))$, where δ_i are the category-dependent radiative corrections, is neglected.
3. Instead of calculating the radiative correction for each of the event categories, with the category-dependent σ_i, we use its average value $\sigma^{\rm smear}_{m_{\tau\tau}}$(CMS). The latter simplification assumes implicitly that:

$$\sum_{i=1}^{38} \sigma_i w_i N_i \approx \sigma^{\rm smear}_{m_{\tau\tau}}({\rm CMS}) \sum_{i=1}^{38} w_i N_i, \qquad (3)$$

where i denotes the event category and N_i the category-dependent number of $Z/\gamma^* \to \tau\tau$ background events satisfying the CMS event-selection criteria. This condition is strictly fulfilled only in the limit of a negligible dispersion of the σ_i values. In reality the dispersion of the σ_i values is 3.1 GeV. This value is sufficiently small to justify such a simplification. In order to quantify such a statement we repeated the calculations for $\sigma^{\rm smear}_{m_{\tau\tau}} = 15$ GeV and for $\sigma^{\rm smear}_{m_{\tau\tau}} = 20$ GeV. The corresponding radiative corrections are found to stay well within the uncertainty range of the radiative corrections which spans the difference between the bare and dressed radiative corrections.

In Fig. 3b we compare our predicted excess of weighted events that originate from the missing QED radiative corrections in the modelling of the $Z/\gamma^* \to \tau\tau$ background with the observed excess of weighted events, taken from the insert of the plot Fig. 3a, and interpreted in Ref. [2] as the Higgs-boson signal. Our predictions are plotted as the shadowed regions, the upper limit corresponding to the dressed radiative corrections and the lower limit corresponding to the bare corrections. As can be deduced from this plot, the missing radiative corrections in the modelling of the $Z/\gamma^* \to \tau\tau$ background could fully account for the excess of events and the Higgs-boson contribution may no longer be required. The p-value qualifying the agreement of the predictions of the excess of events due to the missing radiative corrections in the modelling of the $Z/\gamma^* \to \tau\tau$ background with the data is 0.55. It is calculated for the arithmetic mean of the predictions for the bare and for the dressed radiative corrections with the prediction error taken as a half of the difference of these predictions. The corresponding p-value for the hypothesis in which the Higgs signal is added on top of the missing radiative corrections in the modelling of the $Z/\gamma^* \to \tau\tau$ background is 0.007. Such a hypothesis is clearly disfavoured by the data.

As discussed in Sect. 3.3, a striking footprint of the radiative-corrections-driven excess of events is that it changes sign for $m_{\tau\tau} < M_Z$. This effect, although statistically weak at the present collected luminosity, is indeed observed in the data and well reproduced by the missing radiative corrections in the modelling of the $Z/\gamma^* \to \tau\tau$ background, thus supporting the hypothesis that the excess events may be fully accounted for by the effects of the missing radiative corrections.

4.3 The ATLAS case

Our initial estimate of the effect of the missing radiative correction to the embedding procedure in the modelling of the $Z/\gamma^* \to \tau\tau$ background for the ATLAS analysis presented in Ref. [1] is made separately for the six event categories.

The ATLAS event classes reflect the decay channels of the τ-leptons: $\tau_{lep}\tau_{lep}$, $\tau_{had}\tau_{lep}$ and $\tau_{had}\tau_{had}$. For each of the above three classes, two hadronic remnant configurations, assuring an optimal rejection efficiency of background events with respect to the Higgs-boson signal, are defined: (1) the *Vector-Boson-Fusion (VBF)* configuration, in which the production of the τ-lepton pair is accompanied by the emission of two jets having a large separation in rapidity, (2) the *Boosted* configuration in which the τ-lepton pair recoils against a high transverse-momentum jet(s). The above three decay channels and the two hadronic configurations define six event categories. Additional details about the selection criteria of events belonging to each of the above categories can be found in Ref. [1].

In our initial estimate of the radiative correction effects to the CMS analysis we assume Gaussian smearing of the reconstructed $m_{\tau\tau}$. For the ATLAS case we base our analysis on the published resolution functions presented in Ref. [1] for the VBF and Boosted categories. This allowed us to take into account non-Gaussian resolution tails.

In Fig. 4a, b we compare the ATLAS $m_{\tau\tau}$ distributions for $Z/\gamma^* \to \tau\tau$ decays, for the VBF and Boosted configurations, with the $m_{\tau\tau}$ distribution based on our model of the measurement resolution. The published and our model distributions are in very good agreement which validates our modelling of the experimental resolutions. All the results presented below are be based on this modelling of the experimental resolution. The resolution functions are assumed to be the same for the $\tau_{lep}\tau_{lep}$, $\tau_{had}\tau_{lep}$ and $\tau_{had}\tau_{had}$ decay modes.

The ATLAS selection criteria for the Boosted and VBF categories increase the ratio of the number of accepted $H \to \tau\tau$ events sizeably with respect to the $Z/\gamma^* \to \tau\tau$ background, as compared to the fully inclusive samples. The

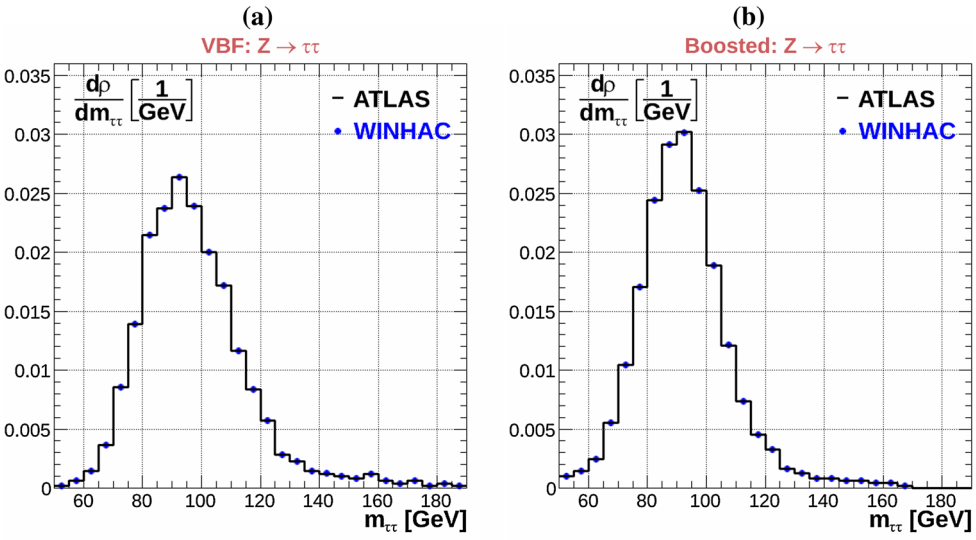

Fig. 4 The reconstructed invariant $\tau^+\tau^-$ mass, $m_{\tau\tau}$, in the ATLAS experiment [1] compared with the WINHAC-based model used in our studies: **a** for the VBF selection of events, and **b** for the Boosted selection of events

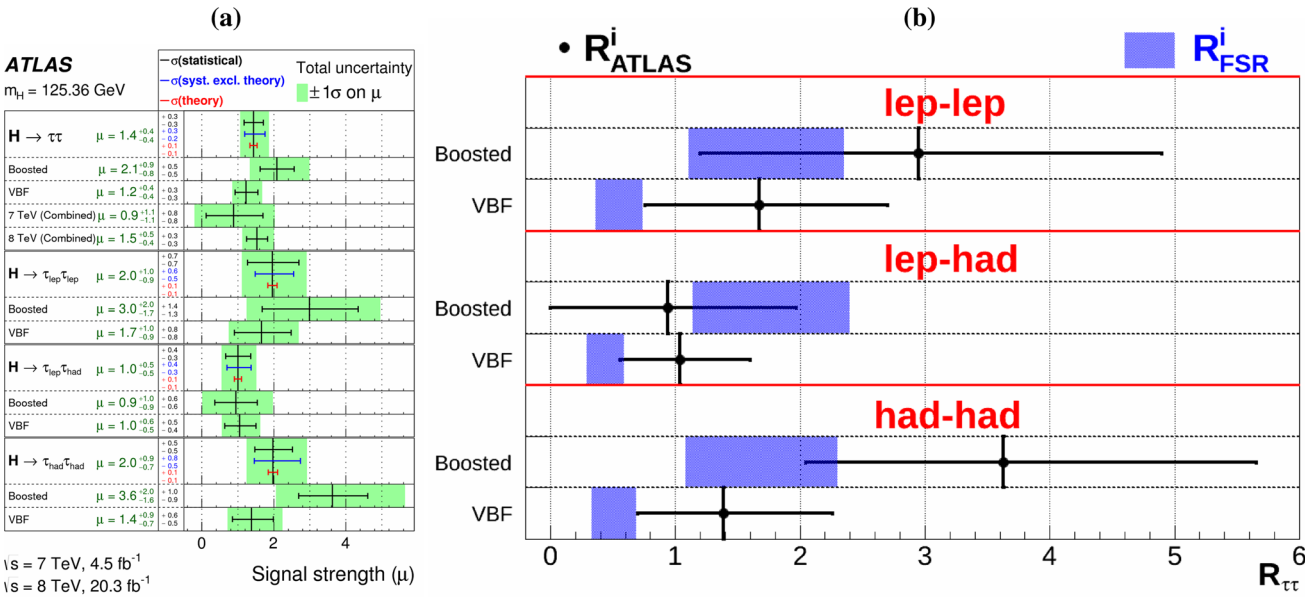

Fig. 5 **a** Reproduction of Fig. 10 taken from the ATLAS paper [1]; **b** a comparison of the $R^i_{\rm ATLAS}$ values taken from Fig. 10 of Ref. [1], with the $R^i_{\rm FSR}$ values for each event category (here, the upper boundaries of the shadowed regions for the $R^i_{\rm FSR}$ values correspond to dressed corrections and the lower boundaries correspond to bare corrections)

ratios of the integrated number of the accepted $H \to \tau\tau$ events, $N^{H,i}_{\rm tot}$, to the number of the accepted $Z/\gamma^* \to \tau\tau$ events, $N^{Z,i}_{\rm tot}$, are determined in our analysis for each event category using Fig. 2 of Ref. [1]. These ratios are used to calculate the corresponding ratios of the event-selection efficiencies in the ATLAS-analysis acceptance region [1]:

$$\frac{\epsilon^i_H}{\epsilon^i_Z} = \frac{N^{H,i}_{\rm tot}}{N^{Z,i}_{\rm tot}} \times \frac{\sigma_Z \times BR(Z \to \tau\tau)}{\sigma_H \times BR(H \to \tau\tau)}, \tag{4}$$

where superscript i denotes the event category. The values of $\sigma_Z \times BR(Z \to \tau\tau)$ and $\sigma_H \times BR(H \to \tau\tau)$ taken from [1] are 1303 and 1.4 pb, respectively. The ratios of the event selection efficiencies are used in turn to calculate the corresponding ratios of the number of excess events that originate from the missing radiative corrections in the modelling of the $Z/\gamma^* \to \tau\tau$ background, to the number of expected excess events from 125 GeV SM Higgs-boson decays in the ATLAS acceptance regions. These ratios, calculated for the $m_{\tau\tau}$ region between 80 and 150 GeV, and denoted as $R^i_{\rm FSR} = N^i_{\rm FSR}/N^i_H$, can be directly compared to the values of the event-category-dependent μ^i parameters, which are the ratios of the observed to predicted Higgs-boson coupling strength to τ-leptons in each event category [1]. This comparison is shown in Fig. 5.

In Fig. 5a we reproduce Fig. 10 taken from the published ATLAS paper [1], which shows the μ^i values for each event category. These values can be interpreted as the event-category-dependent ratios of the number of the observed excess events, with respect to the SM background predictions, N^i_{excess}, to the respective number of events originating from the Higgs-boson decays: $R^i_{\text{ATLAS}} = N^i_{\text{excess}}/N^i_H$, where, as before, i specifies the event category. If the excess of the observed events is produced only by $H \to \tau\tau$ decays, then $R^i_{\text{ATLAS}} = \mu^i = 1$. We refer to this case as *the Higgs-only hypothesis*. If the observed excess of events is fully accounted for by the missing radiative corrections in the modelling of the $Z/\gamma^* \to \tau\tau$ background, $N^i_{\text{excess}} = N^i_{\text{FSR}}$, then $R^i_{\text{ATLAS}} = R^i_{\text{FSR}}$. We refer to this case as the *the FSR-only hypothesis*. Finally, if the observed excess of events is accounted for by contributions from both mechanisms, $R^i_{\text{ATLAS}} = R^i_{\text{FSR}} + 1$. We refer to this case as the *the FSR+Higgs hypothesis*.

In Fig. 5b we compare the values of R^i_{ATLAS} taken from Fig. 5a with the R^i_{FSR} values, for each event category. The upper boundaries of the shadowed regions for the R^i_{FSR} values correspond to dressed corrections and the lower boundaries correspond to bare corrections.

The first observation is that the FSR-only hypothesis provides a satisfactory description of the data – the discrepancy with the data is always less than 1σ and the p-value for this hypothesis is 0.46. Again, as in the CMS case, R^i_{FSR} is calculated for the arithmetic mean of the predictions for the bare and dressed radiative corrections with the prediction error taken as a half of the difference of these predictions. Contrary to the CMS case, for ATLAS the FSR+Higgs hypothesis is the most probable. The p-value for this hypothesis is 0.77, slightly better than for the FSR-only hypothesis. Therefore, although the ATLAS data does not require a contribution from Higgs-boson decays to explain the observed excess of events, a contribution from Higgs-boson decay cannot be ruled out given the level of current experimental uncertainties.

It is intriguing that our prediction for the excess of events originating from the missing radiative corrections in the modelling of the $Z/\gamma^* \to \tau\tau$ background for the preselected VBF samples is about a factor of 2 lower than the prediction for the Boosted samples. A similar effect (at a level of 1σ) is observed in the ATLAS data. The value of R^i_{ATLAS} for the VBF category is also about a factor of 2 lower than that for the Boosted category. This effect calls for a further comment.

Our predictions of the radiative corrections to the embedding procedure for the ATLAS case, in particular the ratio of the size of the effect for the VBF and Boosted categories, rely fully on the ATLAS-analysis-specific efficiencies for the selection of Higgs-decay events in the Monte Carlo signal sample and for the selection of Z/γ^*-boson-decay events in the embedded data sample. In the ATLAS analysis the Monte Carlo events for the VBF Higgs production category are generated with the POWHEG+PYTHIA8 generators [19–23]. As shown in an earlier ATLAS paper [24], devoted to the VBF Z/γ^*-boson production process, both the POWHEG and SHERPA [25] generators fail to describe the data in the phase-space region [24] which is relevant for the analysis presented here. Namely, the Monte Carlo predictions are too high by a factor of $\sim$2 in the region of large two-jet invariant mass (see Fig. 11 in [24]) and should be corrected to obtain the background templates used in extraction of the Z/γ^*-boson VBF signal. Such corrections may also be important for adequate modeling of the Higgs-boson VBF signal. Their absence in the Higgs-boson signal analysis presented in Ref. [1] may explain the apparent discrepancy of the R^i_{ATLAS} and R^i_{FSR} values for the VBF and Boosted categories. If both the Higgs-boson and the Z/γ^*-boson contributions were to be taken from Monte Carlo the impact of these corrections on the ratio of efficiencies for the selection of Higgs decay events and Z/γ^*-boson decay events, would be significantly smaller than in the case of the embedding procedure, and the observed discrepancy may disappear.

4.4 Final remarks

The results presented in this section represent the initial estimation of the size of the radiative corrections to the embedding procedure for the full acceptance regions of the ATLAS and CMS analyses. No attempt is made to determine how the effective corrections would change in more restrictive kinematical regions or for the Boosted Decision Tree (BDT) based analysis, in which all the kinematical properties of the background and signal events are taken into account. Since the BDT analyses of ATLAS and CMS [1,2] are based on distributions which are not corrected for detector effects, we are technically unable to provide the radiative corrections for the BDT-type of analyses. Our analysis shows, however, that the ATLAS and CMS BDT analyses should have taken into account the modifications of the templates of the kinematical distributions for the $Z/\gamma^* \to \tau\tau$ samples caused by the QED radiative corrections to the embedding procedure. This statement holds for the present statistical accuracy of the measurement. For a sizeably larger collected luminosity it may, in principle, be possible to reduce the size of the radiative correction effects by performing the analyses in more severely restricted phase-space regions, in which the impact of radiative corrections is diminished.

5 Embedding procedures and FSR effects

The mechanism in which the missing radiative corrections in the modelling of the $Z/\gamma^* \to \tau\tau$ background could mimic the Higgs-decay signal was communicated by one of the

authors of this paper (MWK) to the authors of [1,2] at the time of preparing these papers for publications. The reply was that the other sources contributing to the uncertainties of the embedding procedure were dominant and the effects of the missing QED radiative correction in the modelling of the $Z/\gamma^* \to \tau\tau$ background are already covered by the corresponding systematic errors. This was claimed to be confirmed by the Monte Carlo studies in which the detector simulation results for the embedded and generated $Z/\gamma^* \to \tau\tau$ samples were compared.

In the subsequent CMS and ATLAS technical papers, following the $H \to \tau\tau$ evidence papers [1,2], more attention has been given, by the respective groups developing the embedding procedures, to the importance of QED radiative effects. In the outlook section of the CMS note devoted to the embedding procedure [26], the importance of quantifying the impact of the final state radiation for various embedding methods was notified but the corresponding studies were left for the future analyses. The ATLAS collaboration published very recently the paper on the embedding procedure [27]. The QED radiative effects were discussed for the first time, jointly with the resolution effects of the reconstructed muon momenta. As a measure of their importance, the distributions of the τ decay lepton transverse momentum and of the invariant mass of the visible $\tau\tau$ decay products, $m_{\tau\tau}^{vis}$, for generator- and detector-seeded τ embedding were presented in Fig. 8a,b of Ref. [27]. These plots demonstrated that the effects of the uncorrected resolution and final-state radiation of the input muons are negligible in the case of reconstructed $\tau\tau$ final states, for which the mass resolution is dominated by the neutrinos produced in the τ decay. This conclusion is indeed correct,[2] but only at a precision level of 5–10 %. However, as our analysis has shown, the extrapolation of such a general conclusion to the Higgs-boson searches, where higher precision is required, cannot be justified.

6 The way forward

As indicated in the previous section, the excess of events attributed to the Higgs signal may be a consequence of the missing QED final-state radiative correction in the modelling of the $Z/\gamma^* \to \tau\tau$ background. In order to discriminate, beyond any doubt, between the three hypotheses formulated in the previous section: FSR-only, Higgs-only and FSR+Higgs, the following experimental tests may provide additional information:

- **The $\mathbf{m}_{\tau\tau}$ dependence test.**
  This test boils down to selecting the event categories for which the experimental resolution of the reconstructed $m_{\tau\tau}$ is the best, say in the 10 GeV $\leq \sigma_{m_{\tau\tau}}^{\text{smear}} \leq$ 15 GeV range, and to performing the analysis in two subsamples of events selected below and above $m_{\tau\tau} = 120$ GeV. If the excess of events is found to be confined to the lower mass region, the FSR-only hypothesis is favoured. If it is found to be concentrated in the higher mass region, the Higgs-only hypothesis is more likely.
- **The embedded τ momentum definition test.**
  Here we exploit the fact that most of the large energy photons radiated by the outgoing muons coming from Z/γ^*-boson decays are collinear with the initial (vertex) outgoing muon direction. The identification of FSR photons is easier thanks to the solenoidal magnetic field in both the ATLAS and CMS experiments. The FSR photon energy clusters reconstructed in the electromagnetic calorimeter can be differentiated (with a certain efficiency) from the muon energy loss in the calorimeters because of the bending of the muons in the magnetic field. If the energy of the identified radiative photon clusters is added to muon energy which is measured by its track, the size of the radiative correction to the embedding procedure is drastically reduced. Such a test can be done in particular for the VBF subsample of events, for which the transverse momentum spectrum of muons is softer than for the Boosted sample. Here the larger deflection in the magnetic field allows for larger separation of the radiative photon clusters and the muon energy deposition from muon interactions in the material in the electromagnetic calorimeter. By varying the association criteria of electromagnetic clusters with the muon, one can experimentally control the level of the radiative corrections to the embedding procedure in the modelling of the $Z/\gamma^* \to \tau\tau$ background.
  For higher energy muons one could add all the energy deposition in the electromagnetic calorimeter to the energy of the muon measured by tracking, and perform a statistical subtraction of the energy deposition component that results from direct muon interactions in the material of the electromagnetic calorimeter. The statistical subtraction can utilize a spectrum of energy deposition simulations for muons of different momenta.
- **The bare-versus-dressed τ-lepton test.**
  As shown in Fig. 2, the size of the radiative corrections to the embedding procedure is different for these two definitions of the outgoing τ-lepton momentum. In the majority of τ-lepton decays the radiative photons cannot be experimentally resolved and they are included in the

[2] Note, that Fig. 8a of Ref. [27] is largely irrelevant to the studies of the radiative effects because hard-photon radiation affects predominantly the transverse momentum distribution of the sub-leading rather than the leading lepton. Moreover, the negative slope of the distribution of the visible $\tau\tau$ mass shown in Fig. 8b is clearly visible even at the 5–10 % precision level of the studies presented in [27]. This negative slope may be considered as a footprint of the importance of the FSR effects.

momentum reconstruction of the dressed τ-lepton. However, as far as the embedding procedure is concerned, the radiation and decays of τ-leptons are generated by Monte Carlo programs in which the source of each photon is clearly defined. The test would consist of repeating the embedding analysis twice, for the dressed and for the bare τ-lepton definitions. If the main source of the excess of "Higgs-like" events are the radiative corrections to the embedding procedure, this excess would vary in a predictable way, and the FSR-only and Higgs-only hypotheses could be discriminated with respect to each other.

– **The selection efficiency test.**
The size of the radiative corrections to the embedding procedure depends very strongly on the relative efficiency of selecting the Higgs-like events with respect to the remaining background, in optimal restricted phase-space volumes. The embedding procedure, in which the main background is determined directly from the data, while the Higgs signal is simulated using the Monte Carlo generated events, is prone not only to the QED radiative corrections, but also to the QCD radiative corrections, which are treated differently for data and Monte Carlo events. The test would consist of determining the ratio, rather than absolute values, of the selection efficiencies in a restricted kinematical region from a fixed Monte Carlo generator, having the same QCD approximations for the production of Z/γ^* and Higgs bosons. The large uncertainties of the absolute predictions cancel in this ratio. This test is of particular importance in view of the apparent discrepancy of the $R^i_{\rm FSR}$ and $R^i_{\rm ATLAS}$ values between the VBF and Boosted samples of events. The $R^i_{\rm FSR}$ values are driven by the ratio of efficiencies, as illustrated in Eq. (4), while the $R^i_{\rm ATLAS}$ values carry, in addition, an imprint of the relative strength of the Higgs-boson couplings to fermions and bosons. A single-Monte-Carlo-based measurement could be decisive for an unambiguous interpretation of the "VBF vs. Boosted" discrepancy.

7 Conclusions

In this paper we present an analysis of the effects of QED final-state radiative corrections to the modelling of the $Z/\gamma^* \to \tau\tau$ process, which is the dominant background in the $H \to \tau\tau$ searches. We focus our attention on the radiative corrections to the embedding procedure used by ATLAS and CMS to model the $Z/\gamma^* \to \tau\tau$ background in the extraction of the $H \to \tau\tau$ signal from experimental data. We make an initial estimate of the size of these corrections for the ATLAS and CMS analyses [1,2] and show that the missing radiative corrections in the embedding procedure may explain the excess of events which has been attributed to a Higgs-boson signal. We propose several experimental tests which can differentiate between an excess which originates from missing QED radiative corrections in the modelling of the $Z/\gamma^* \to \tau\tau$ background and an excess originating from Higgs-boson decays.

The goal of this paper is to re-draw the attention of the CMS and ATLAS collaborations to the importance of the effect of the QED radiative corrections to the embedding procedure for modelling the $Z/\gamma^* \to \tau\tau$ background. Our earlier suggestions on this matter, addressed to the ATLAS and CMS collaborations at the time of preparation of their respective papers, are now quantified by an initial estimate of the size of the effect. It is our hope that these estimates will persuade both collaborations to take into account the QED radiative corrections to their respective embedding procedures used to model the $Z/\gamma^* \to \tau\tau$ background in the extraction of the $H \to \tau\tau$ signal from current and future experimental data.

Acknowledgments We would like to thank T. Przedziński and Z. Wąs for their help in interfacing PHOTOS to WINHAC. We acknowledge the help of the Academic Computer Centre CYFRONET AGH in Krakow, Poland, where our numerical simulations were performed with the use of the computing cluster Zeus. We would like to thank Anne Pfost and Patrick Czodrowski for their critical reading of the manuscript.

Funded by SCOAP[3].

References

1. G. Aad et al. (ATLAS Collaboration), JHEP **1504**, 117 (2015). arXiv:1501.04943 [hep-ex]
2. S. Chatrchyan et al. (CMS Collaboration), JHEP **1405**, 104 (2014). arXiv:1401.5041 [hep-ex]
3. W. Płaczek, S. Jadach, WINHAC version 1.37: The Monte Carlo event generator for single W-boson production with leptonic decays in hadron collisions. http://cern.ch/placzek/winhac
4. W. Płaczek, S. Jadach, Eur. Phys. J. C **29**, 325 (2003). arXiv:hep-ph/0302065
5. W. Płaczek, PoS **EPS-HEP2009**, 340 (2009). arXiv:0911.0572 [hep-ph]
6. W. Płaczek, S. Jadach, M.W. Krasny, Acta Phys. Pol. B **44**, 2171 (2013). arXiv:1310.5994 [hep-ph]
7. M.R. Whalley, D. Bourilkov, R.C. Group, The Les Houches accord PDFs (LHAPDF) and LHAGLUE, in *HERA and the LHC: a workshop on the implications of HERA for LHC physics. Proceedings, Part B*. European Organization for Nuclear Research (2005). arXiv:hep-ph/0508110
8. E. Barberio, Z. Wąs, Comput. Phys. Commun. **79**, 291 (1994)
9. P. Golonka, Z. Wąs, Eur. Phys. J. C **45**, 97 (2006). arXiv:hep-ph/0506026
10. P. Golonka, Z. Wąs, Eur. Phys. J. C **50**, 53 (2007)

11. N. Davidson, T. Przedzinski, Z. Wąs, Comput. Phys. Commun. **199**, 86 (2016). arXiv:1011.0937 [hep-ph]
12. A.B. Arbuzov, R.R. Sadykov, Z. Was, Eur. Phys. J. C **73**(11), 2625 (2013). arXiv:1212.6783 [hep-ph]
13. T. Sjostrand, S. Mrenna, P. Skands, JHEP **05**, 026 (2006). arXiv:hep-ph/0603175
14. M.W. Krasny, W. Płaczek, Acta Phys. Pol. B **43**, 1981 (2012). arXiv:1209.4733 [hep-ph]
15. D. Stump, J. Huston, J. Pumplin, W.K. Tung, H.L. Lai, S. Kuhlmann, J.F. Owens, JHEP **0310**, 46 (2003). arXiv:hep-ph/0303013
16. A.D. Martin, W.J. Stirling, R.S. Thorne, G. Watt, Eur. Phys. J. C **63**, 189 (2009). arXiv:0901.0002 [hep-ph]
17. S. Jadach, Z. Wąs, B.F.L. Ward, Comput. Phys. Commun. **130**, 260 (2000). Source code available from http://home.cern.ch/jadach/
18. T.K.O. Doan, W. Płaczek, Z. Wąs, Phys. Lett. B **725**, 92 (2013). arXiv:1303.2220 [hep-ph]
19. P. Nason, JHEP **0411**, 40 (2004). arXiv:hep-ph/0409146
20. S. Frixione, P. Nason, C. Oleari, JHEP **0711**, 70 (2007). arXiv:0709.2092 [hep-ph]
21. S. Alioli, P. Nason, C. Oleari, E. Re, JHEP **1006**, 43 (2010). arXiv:1002.2581 [hep-ph]
22. E. Bagnaschi, G. Degrassi, P. Slavich, A. Vicini, JHEP **1202**, 88 (2012). arXiv:1111.2854 [hep-ph]
23. T. Sjöstrand, S. Mrenna, P. Skands, Comput. Phys. Commun. **178**, 852 (2008). arXiv:0710.3820 [hep-ph]
24. G. Aad et al. (ATLAS Collaboration), JHEP **1404**, 31 (2014). arXiv:1401.7610 [hep-ex]
25. T. Gleisberg et al., JHEP **0902**, 7 (2009). arXiv:0811.4622 [hep-ph]
26. B. Treiber, Abschazung des Untergrundes aus $Z \to \tau\tau$ Ereignissen in $Z \to \tau\tau$ Analysen, Karlsruhe Institute of Technology preprint, IEKP-KA/2015, 30 Juli 2015
27. G. Aad et al. (ATLAS Collaboration), JINST **10**(09), P09018 (2015). arXiv:1506.05623 [hep-ex]